Title	A simple fracture mechanical interpretation of size effects in concrete fracture toughness tests
Author(s)	Kim Wallin
Citation	Engineering Fracture Mechanics vol. 99(2013), pp. 18 - 29
Date	2013
URL	http://dx.doi.org/10.1016/j.engfracmech.2013.01.018
Rights	This article may be downloaded for personal use only.

A SIMPLE FRACTURE MECHANICAL INTERPRETATION OF SIZE EFFECTS IN CONCRETE FRACTURE TOUGHNESS TESTS

Kim Wallin

VTT Materials and Built Environment,

P.O. Box 1000, FI-02044 VTT, Espoo, Finland

Tel:+358 50 511 4126

Kim.Wallin@vtt.fi

ABSTRACT

Concrete is a so called quasibrittle material which, despite predominantly elastic material response, exhibits in tension loading a stable non-linear fracture response, when tested under displacement control. The reason for the non-linearity is the development of a fracture process zone, in front of the crack, due to micro-cracking and crack bridging. The effect of the fracture process zone is to make the specimen sense the crack as being longer than $a_0+\Delta a$. The fracture process zone causes thus an effective increase in the crack driving force and apparent fracture resistance. Here, a novel LEFM based estimate of the effective stress intensity factor and the effective crack growth at maximum load in a fracture mechanics test is used to obtain a simple power law approximation of the effective K-R curve. It is shown that it is applicable to the description of not only different size specimens, but also specimens with varying geometry. The method is based on a new theoretical estimate of the effective crack growth corresponding to maximum load.

KEYWORDS

Concrete fracture, size effect, fracture toughness, quasibrittle materials, K-R curve.

NOMENCLATURE

a	Crack length
a_0	Initial crack length
a_{0e}	Effective initial crack length for an unnotched specimen
B	Specimen thickness
c	Constant related to specimen geometry
C	Constant in Bažant size effect expression
C(T)	Compact tension specimen
DEC(T)	Double edge cracked tension specimen
H	Compact tension specimen width
G	Energy release rate
K	Stress intensity factor
K_{IC}	Fracture toughness for a completely brittle material
K_{Ieff}	Effective stress intensity factor corresponding to $a_0 + \Delta a_{eff}$
K_{1mm}	Stress intensity factor corresponding to 1 mm crack growth [$N/mm^{3/2}$]
K-R curve	Dependence between stress intensity factor and crack growth (K_{Ir})
m	Power in power law expression for effective K-R curve
P	Load
P_{max}	Maximum load
PZ	Active fracture process zone
S	Span width in SE(B) specimen
SE(B)	Single edge cracked bend specimen
W	Specimen height
W_0	Normalising constant
Δa	Crack growth
Δa_{eff}	Effective crack growth
$\Delta a_{effPmax}$	Effective crack growth corresponding to maximum load
σ_f	Tensile stress
σ_{nomW}	Nominal stress for specimen height W

1 INTRODUCTION

Concrete is a so called quasibrittle material which, despite predominantly elastic material response, exhibits in tension loading a stable non-linear fracture response, when tested under displacement control (Fig. 1 [1]). The reason for the non-linearity is the development of a fracture process zone, in front of the crack, due to micro-cracking and crack bridging. An excellent review of the physical fracture process of concrete has been given in e.g. [2] and need not be covered here in any more detail. Here, the focus is on the fracture mechanical description of the effect of the fracture process zone on the structural behaviour of the test specimen and prediction of size effects.

The cracking of concrete is schematically presented in Fig. 2. The shaded area in Fig. 2, relates to the micro-cracked material. The part of the micro-cracked material, lying in front of the macroscopic crack (including initial crack length a_0 and extended crack Δa), constitutes the active fracture process zone. In this region the material cohesion is weakened due to the micro-cracking. The effect of the fracture process zone is to make the specimen sense the crack as being longer than $a_0+\Delta a$. The fracture process zone causes thus an effective increase in the crack driving force. The effect of the fracture process zone is similar in nature to the Irwin plasticity correction [3] for metals.

The part of the micro-cracked material that becomes engulfed in the crack wake, is no longer actively affecting the crack driving force, but it has absorbed energy related to the micro-crack surfaces. This has the effect of increasing the materials effective fracture resistance (Fig. 3).

Often, fracture toughness tests of concrete are actually assessed by estimating an effective stress intensity factor and effective crack length [4], to derive an effective K-R curve in line with the ASTM E561 – 10 test standard [5]. This procedure is still, however, not widely used, partly due to the question regarding the significance of the effective crack length and effective crack driving force. Another method called the double-K or double-G criterion is based on the estimate of the stress intensity at the onset of first crack extension (with a non-developed fracture process zone) and the stress intensity corresponding to maximum load in the test [4]. This method is really an improvement of the classical tests where the maximum load has been combined with the initial crack length (a_0) to obtain a nominal fracture toughness value. The challenge with the double-K criterion lies in the reliable detection of the moment of crack initiation, which is almost invisible on the load-displacement record. Also, the estimation of the crack length at maximum load contains an experimental challenge and the necessity to combine both estimates of the crack tip displacement

and load displacement. This prevents the method from becoming a simple quality assurance type of fracture toughness estimate.

As a compromise to the use of the classical nominal load maximum stress intensity factor, a special size effect expression has been proposed by Bažant. (See e.g. [6]). The Bažant size effect expression is versatile and has been shown to describe well the size effect in load maximum values of concrete and other quasibrittle materials. The Bažant size effect expression for load maximum (P_{max}) can be expressed in the form of Eq. (1). B and W denote the fracture toughness specimen thickness and width and σ_f corresponds to the tensile stress of the material. The constant c accounts for specimen geometry and W_0 is a normalising constant. The constants c and W_0 are determined by fitting to test results from different size specimens of identical geometry. Apparently the only weakness with the size effect expression is that a comparison between different loading geometries is not possible without the inclusion of additional fitting parameters [7].

$$\frac{P_{\max}}{B \cdot W} = \frac{c \cdot \sigma_f}{\sqrt{1 + \frac{W}{W_0}}} \tag{1}$$

Here, a LEFM based estimate of the effective stress intensity factor and the effective crack growth at maximum load in a fracture mechanics test is used to obtain a simple power law approximation of the effective K-R curve that is applicable to the description of not only different size specimens, but also specimens with varying geometry.

2 FRACTURE MECHANICAL ESTIMATE OF MAXIMUM LOAD

In the case of metals, the materials tearing resistance is usually well described with a simple power law expression. Assuming, that the evolution of the fracture process zone and its effect on the effective materials fracture resistance behaves similarly to metals, also the effective stress intensity factor as a function of the effective crack growth should be possible to approximate with a power law in the form of Eq. (2).

$$K_{Ieff} \approx K_{1mm} \cdot \Delta a_{eff}^{m} \tag{2}$$

For metals, when the tearing resistance is expressed in J-integral units, the power m is close to 0.5 or less. Thus, in K units the power should be in the vicinity of 0.25. If the fracture process zone size

is very small compared to the crack growth, Δa, the power m will be small. If it is large compared to Δa, the power m should be closer to 0.25 or even above. When the relation between crack growth and fracture process zone no longer exists, the power m is expected to grow uncontrollable. This is not, however, expected to occur until well beyond the maximum load value.

The effective stress intensity factor is related to load and the effective crack length by Eq. (3).

$$K_{Ieff} = \frac{P}{B \cdot \sqrt{W}} \cdot f\left(\frac{a_0 + \Delta a_{eff}}{W}\right) \tag{3}$$

Eq. (3) differs from the classically used nominal stress intensity factor, which is calculated using only the initial crack size (a_0). The nominal stress intensity factor under-predicts the true effective crack driving force and should not be used in the assessment of quasibrittle materials.

Combining Eqs. (2) and (3) leads to a relation between load and effective crack growth, Eq. (4).

$$P = \frac{K_{1mm} \cdot \Delta a_{eff}^{m} \cdot B \cdot \sqrt{W}}{f\left(\frac{a_0 + \Delta a_{eff}}{W}\right)} \tag{4}$$

When the derivative of Eq. (4) (dP/da) is 0, the load and effective crack length correspond to maximum load. This leads to the relation between power m and effective crack extension in the form of Eq. (5) [8].

$$m = \frac{\Delta a_{effP\max}}{W} \cdot \frac{f'\left(\frac{a_0 + \Delta a_{effP\max}}{W}\right)}{f\left(\frac{a_0 + \Delta a_{effP\max}}{W}\right)} \tag{5}$$

Eq. (5) is general and can be applied to any geometry for which the shape function f(a/W) is known. A numerical inversion of Eq. (5) is quite simple. One can tabulate a set of a_0, m and $\Delta a_{effPmax}$ values for a desired geometry and then a specific equation may be fitted to the data, or the information can be interpolated from the table. As an example, the solutions for the standard SE(B) and C(T) specimens are shown graphically in Figs 4a and b. An approximate solution for the standard SE(B) specimen with span width S/W = 4 is given by Eq. (6) and for the standard C(T) specimen with H/W = 0.6 is given in Eq. (7).

$$\frac{\Delta a_{effP\max}}{W} \approx \frac{0.001118 + \left(\frac{a_0}{W}\right)^2 \cdot m - \left(\frac{a_0}{W}\right) \cdot m}{0.3886 \cdot \mathrm{m} - 0.1963 - \left(\frac{a_0}{W}\right) - 2.147 \cdot \left(\frac{a_0}{W}\right) \cdot \mathrm{m}} \qquad \left[\frac{S}{W} = 4, \frac{a_0}{W} \geq 0.1\right] \tag{6}$$

$$\frac{\Delta a_{effP\max}}{W} \approx \frac{m \cdot \sqrt{\frac{a_0}{W}}}{0.1542 + 8.063 \cdot \left(\frac{a_0}{W}\right)^2 \cdot m + exp\left\{2.94 \cdot \left(\frac{a_0}{W}\right)^2\right\} - 0.8219 \cdot m} \qquad \left[\frac{H}{W} = 0.6, \frac{a_0}{W} \geq 0.1\right] \tag{7}$$

It is important to note that Eqs. (6) and (7) are applicable only for standard specimen geometries. Especially in the case of the SE(B) specimen often different S/W ratios are used in the tests. For such tests, the standard f(a/W) expression can be adjusted e.g. by Eq. (8) [9] to be used together with its derivative in Eq. (5).

$$\mathrm{f}\left(\frac{\mathrm{a}}{\mathrm{W}}\right)_{\mathrm{S/W}} = \mathrm{f}\left(\frac{\mathrm{a}}{\mathrm{W}}\right)_{\mathrm{S/W=4}} \cdot \left\{1 + \left(1 - \frac{4\mathrm{W}}{\mathrm{S}}\right)\left(0.08\left(1 - \frac{\mathrm{a}}{\mathrm{W}}\right) + 0.24\left(1 - \frac{\mathrm{a}}{\mathrm{W}}\right)^2 - 0.28\left(1 - \frac{\mathrm{a}}{\mathrm{W}}\right)^3\right)\right\} \tag{8}$$

The analysis consists of solving the power m and K_{1mm} iteratively by combining Eqs (4) and (5) to provide the correct maximum load values for different size and/or geometry specimens. The result is obtained in the form of the effective K-R curve in the form of Eq. (2) which then can be used for the evaluation of other geometries.

For a constant geometry and fixed initial crack size ratio (a_0/W), the effective crack growth is directly related to the specimen width (W). This makes a comparison with the Bažant size effect expression quite simple. When the Bažant size effect expression is written in the form of maximum load stress ratio for 2 specimen widths (W_1 and W_2), the result can be expressed in the form of Eq. (9). The corresponding K-R curve size effect can be expressed in the form of Eq. (10). The two size effects are compared graphically, for realistic values of the constants C and m in Fig. 5. The difference between the two size effects is strikingly small, within realistic experimental size ranges.

$$\frac{\sigma_{nomW1}}{\sigma_{nomW2}} = \left(\frac{C + \frac{W_1}{W_2}}{C + 1}\right)^{-0.5} \tag{9}$$

$$\frac{\sigma_{nomW1}}{\sigma_{nomW2}} = \left(\frac{W_1}{W_2}\right)^{m-0.5} \tag{10}$$

Next, the two size effect expressions are compared on actual test data.

3 ASSESSMENT OF MAXIMUM LOAD DATA

Fig. 6 shows maximum load data as a function of specimen size for self-similar concrete and mortar specimens [7]. When accounting for the effective crack growth at maximum load, the effective stress intensity factor K-R curve can be fitted to the maximum load data. The result is shown as the solid line in Fig. 6. The Bažant size effect fit to the data is shown as a dashed line. The two descriptions of the two data sets are practically indistinguishable. Two differences between mortar and concrete can be seen from the analysis. The power m is much smaller for the mortar than for the concrete. This indicates that the facture process zone for mortar is clearly smaller and less dependent on loading level than for concrete. This is likely due to a bridging cohesive stress of coarse aggregates in concrete, which increases the size of the fracture process zone and enhances the power m. On the other hand is K_{1mm} smaller for concrete than mortar. Physically, K_{1mm} represents more the pure fracture toughness of the material, without the enhancing effect of the fracture process zone. This value is smaller for concrete than for mortar, possibly due to a higher density of mortar than concrete, but another reason is also possible. The overall effect is that for small specimens mortar shows a higher maximum load than concrete, whereas the relation is reversed for large specimens.

Fig. 7 shows maximum load data and resulting effective K-R estimates for sound and degraded self-similar concrete specimens of different size [10]. Similarly to before, the K-R curves were fitted to the maximum load data, accounting for the effective crack growth at maximum load. Also here, for all three cases, the K-R curve size effect and the Bažant size effect are practically indistinguishable. The effect of the Calcium Leaching degradation is mainly to lower the K-R curves, i.e. decrease the facture process zone size (Fig. 7d). All three conditions show closely similar initiation behaviour, whereas the leached conditions show smaller m values, indicating a smaller fracture process zone. This is connected to the cohesive zone characteristics of the process zone, but the physical reason is unknown.

Fig. 8 shows maximum load data for C(T) specimens of different size and thickness, but with a constant initial crack length ratio [11]. Because the specimen thickness varies, the load is normalised with the thickness to clarify the effect of specimen width on the maximum load. The

effective K-R curve, based on the effective crack growth at maximum load described the data well. Again, the K-R curve size effect and the Bažant size effect are practically indistinguishable.

The above examples dealt with self-similar specimens with a constant initial crack length ratio. Fig. 9 shows two data sets for constant size SE(B) specimens with varying crack length. Fig. 9a corresponds to standard specimens with S/W = 4 [12], whereas Fig. 9b refers to four point bending specimens corresponding to pure bending [13]. In both cases, the effective K-R curve describes the maximum load very well.

Fig. 10a compares the maximum load for four different specimen sizes with four different initial crack lengths [2]. All the different maximum load $K_{Ieff} - \Delta a_{eff}$, data pairs fall on a common power-law curve (Fig. 10b). Thus, a single effective K-R curve describes both the size effect as well as the effect of crack length. Another example of this is shown in Fig 11, where varying crack length data from three different specimen sizes [14] are shown to be well described with a single effective K-R curve. Originally the smallest specimen size data was discarded as representing incomparable data due to a too small specimen size. Therefore the power law effective K-R curve was only fitted to the two larger specimen sizes. However, the use of the effective K-R curve describes well all three specimen sizes. Fig. 11 includes also another "small" specimen data set [15] representing the same type of concrete. The points denoted as squares with crosses lie very close to the other "small" specimen data (open squares), indicating that the fracture toughness of the concretes is similar.

These examples show the descriptive power of the power law effective K-R curve estimated based on the maximum load values. The validity and the restriction of the method are discussed next.

4 DISCUSSION

The proposed method relies on the assumption that the effective K-R curve up to maximum load can be approximated by a simple power law. Karihaloo and Nallathambi [16] collected a large number of SE(B) data and estimated from the experimental load-displacement traces, the relation between initial crack length and the effective (based on effective compliance) crack length corresponding to maximum load. Their results have been reproduced in Fig. 12. Included in the figure are theoretical estimates from Eq. (6) for the m values 0.1 and 0.45. It should be pointed out that the theoretical estimates are for a fixed span width of S/W = 4, whereas the Karihaloo and Nallathambi data contains specimens with varying span widths. A shorter span width increases the shear stresses in the specimen, having the effect of increasing the size of the fracture process zone.

This translates into a larger m value. Overall, the Karihaloo and Nallathambi data provides a strong validation of Eq. (6) and the assumption that the effective K-R curve up to maximum load can be approximated by a simple power law.

Even though the effective K-R curve describes well the specimen size and crack length effect, it does not mean that it would be insensitive to constraint effects. A low-constraint geometry will have the effect of increasing the size of the fracture process zone, thus increasing the effective fracture toughness. An example of this is shown in Fig. 13 [7], where different size double edge cracked tensile specimens for concrete and mortar, with a constant initial a_0/W ratio, are analysed by the effective K-R curve method. The materials are the same as shown in Fig. 6 for SE(B) specimens. As can be expected, the Bažant size effect and the K-R curve size effect produce a similar description of the size effect. However, comparison to Fig. (6) shows an important difference in the K-R curve description. The K_{Ieff} corresponding to an effective crack growth of 1 mm is only little affected by the specimen type. The power m is, however, clearly larger for the DEC(T) specimens than for the SE(B) specimens. The relative behaviour between concrete and mortar is however unaffected. This example highlights the strong effect of loading mode on the fracture process zone development.

In a cracked specimen, the fracture process zone size is initially controlled by the effective stress intensity factor connected to the crack. In an uncracked (plain) specimen the fracture process zone size will be controlled by the overall stress distribution. In a bend specimen, the stresses change relative to the width. Thus it is expected that the fracture process zone in a plain bend specimen behaves like a proportionally sized crack. This was investigated in Fig. 14, with maximum load data for different size SE(B) specimens corresponding to cracked ($a_0/W = 1/3$) and uncracked specimens [17]. The effective K-R curve was first fitted to the cracked specimens and then, the resulting power law was used to predict the maximum loads for the uncracked specimens. Assuming an effective initial crack length of $a_{0e}/W = 0.035$ provides an excellent description of the uncracked specimen data. This means that, when the crack starts macroscopically to grow in the uncracked specimens, the effective crack length due to the partially damaged fracture process zone is $0.035 \cdot W$. The power m, is not affected emphasizing that the effective power law K-R curve, to a large extent, is the product of the fracture process zone evolution.

The effective K-R curve describes well the specimen behaviour up to maximum load. This is exemplified in Fig. 15, where SE(B) data for limestone is analysed. Fig. 15a, shows the maximum load values for self-similar specimens of different size [18]. Even though limestone differs from

concrete, the fracture process is sufficiently similar to enable the use of limestone as an example. The power law K-R curve was fitted to the maximum load data in Fig. 15a. Then, the K-R curve estimate was used to predict the load displacement up to maximum load for the three different specimen sizes (Figs 15b,c,d). For the prediction, the crack is first advanced several small steps of Δa_{eff}. Next the K-R curve is used to estimate the K_{Ieff} and P corresponding to a + Δa_{eff}. Finally the estimated load is used to calculate the displacement corresponding to a + Δa_{eff}, from the theoretical compliance. Considering the scatter of individual load-displacement traces, the prediction up to maximum load is excellent. Thus, this very simple power law K-R procedure can be used to predict the non-linearity in concrete and stone structures up to maximum load.

Beyond maximum load, the connection between the effective crack length and the fracture process zone size breaks up. This is highlighted in Fig. 16 where concrete specimens, whose maximum load data were presented in Fig. 7a. The load-displacement data was extracted from [1], so that for each specimen size representative upper and lower bound load-displacement traces were digitised. The effective crack length was estimated directly from the individual load-displacement data pairs, assuming that all the non-linearity is due to effective crack growth. Fig. 16a shows the effective crack driving force versus absolute effective crack growth and Fig. 16b shows the effective crack driving force versus proportional crack growth. Also included in the plots is the effective K-R curve estimated for the maximum load values in Fig. 7a. It is seen that for crack growth up to maximum load and slightly beyond, the effective K-R curve follows the absolute effective crack growth, whereas for large crack growths the effective K-R curve follows the proportional effective crack growth. This is a direct result of the fracture process zone evolution. Prior to maximum load, the fracture process zone is controlled by the fracture mechanical loading introduced by the crack. At some point, the connection between process zone size and the effective crack length breaks up. Finally, when the facture process zone has fully engulfed the crack and possibly extended to the free surface, the fracture process zone size develops as if there was no single crack in the structure.

The present method is not in all respects entirely new. The assessment method proposed e.g. by Bažant [19] contains similarities to the power law K-R curve, in the respect of trying to estimate the amount of effective crack growth at maximum load. The use of the power law curve shape to describe the effective crack driving force versus effective crack length and the resulting theoretical estimate of the effective crack growth at maximum load is, however, unique. In all, the proposed power low K-R procedure can be regarded as a simplification to the method proposed in [19]. The power law method contains also similarities to an analytical cohesive zone method, which has been applied to describe the size effect in SE(B) specimens [20, 21]. The power law method is, however,

much easier to use and provides an at least as good description of the size effect as can be seen by comparing Fig. (11) with Figs (4-6) in [21]. The advantage of the power law procedure lies in the very simple quantification of the fracture process zone development. A small power m indicates a brittle material, where the fracture process zone remains small throughout the fracture process. This is the case for m values of the order of 0.1 and below. The other extreme is a large m value in which case the material is crack insensitive and the damage comes mainly from the fracture process zone evolution. The method enables also the quantification of constraint in terms of the power m.

The procedure results in the estimate of the effective stress intensity factor corresponding to 1 mm effective crack growth. This parameter is easily correlated to the initiation toughness estimated in the double-K criterion test [4]. For example, for the 160 mm specimens in Fig. 11, Xu and Reinhardt [4] have estimated the average initiation toughness to be 26.7 N/mm$^{3/2}$ and for the 320 mm specimens 24.6 N/mm$^{3/2}$. This compares nearly exactly with the 1 mm value of 24.8 N/mm$^{3/2}$ obtained for the combined analysis of the two specimen sizes as shown in Fig. 11.

5 SUMMARY AND CONCLUSIONS

Concrete is a so called quasibrittle material which, despite predominantly elastic material response, exhibits in tension loading a stable non-linear fracture response, when tested under displacement control. The reason for the non-linearity is the development of a fracture process zone, in front of the crack, due to micro-cracking and crack bridging. The effect of the fracture process zone is to make the specimen sense the crack as being longer than $a_0+\Delta a$. The fracture process zone causes thus an effective increase in the crack driving force and apparent fracture resistance. The fracture modelling of concrete has been considered a mature theory. However, Present state of the art testing and assessment methods are somewhat cumbersome to use. Here, a LEFM based estimate of the effective stress intensity factor and the effective crack growth at maximum load in a fracture mechanics test is used to obtain a simple power law approximation of the effective K-R curve. It is shown that it is applicable to the description of not only different size specimens, but also specimens with varying geometry. The method is based on a new theoretical estimate of the effective crack growth corresponding to maximum load.

It can be concluded that:

- The presented procedure results in a simple two parameter description of the effective fracture resistance of quasibrittle materials.

- The procedure describes the specimen size effect on maximum load values with equal accuracy to the Bažant size effect expression.
- The procedure describes the effect of initial crack length on the maximum load values.
- The procedure enables the construction of the load-displacement dependence up to maximum load.
- The procedure enables a simple classification of the materials fracture process zone evolution.
- The procedure can be used in the context of the so called double-K criterion to describe the effective initiation toughness value.
- The procedure can be used to examine constraint effects on the materials fracture process zone evolution.
- In the future, the procedure may be used to assist damage mechanics type modelling of the failure of quasibrittle materials.

6 ACKNOWLEDGEMNTS

This work has been part of the FAR project belonging to the SAFIR 2014 research programme funded by VTT and by the State Nuclear Waste Management Fund (VYR), as well as other key organisations. The present work is connected to the quantification of constraint effects in brittle and quasibrittle materials.

REFERENCES

1 Le Bellégo C, Dubé JF, Pijaudier-Cabot G, Gérard B. Calibration of nonlocal damage model from size effect tests. European Journal of Mechanics A/Solids 2003;22:33–46.

2 Kumar S,·Barai SV. Concrete fracture models and applications. Berlin Heidelberg: Springer-Verlag; 2011.

3 Irwin GR. Plastic zone near a crack and fracture toughness. Sagamore Research Conference Proceedings, Vol. 4, 1961.

4 Xu S, Reinhardt HW. Determination of double-K criterion for crack propagation in quasibrittle materials, Part II: Analytical evaluating and practical measuring methods for three-point bending notched beams. Int J Fract 1999;98:151–77.

5 ASTM E561 – 10. Standard Test Method for K-R Curve Determination. Annual book of standards, Volume 03.01. ASTM International West Conshohocken, PA 2011.

6 Bažant ZP, Planas J. Fracture and size effect in concrete and other quasibrittle materials. Florida: CRC Press; 1998.

7 Bažant ZP, Pfeiffer PA. Determination of fracture energy from size effect and brittleness number. ACI Materials Journal 1987;84:463-80.

8 Wallin KRW. Critical assessment of the standard ASTM E 399. J ASTM Int 2005;2.

9 Wallin K. Fracture toughness of engineering materials - estimation and application. Warrington UK: EMAS Publishing; 2011.

10 Le Bellego C, Gérard B, Pijaudier-Cabot G. Chemomechanical effects in mortar beams subjected to water hydrolysis. J Engrg Mech ASCE 2000;126:266–72.

11 Zhang X, Xu S. A comparative study on five approaches to evaluate double-K fracture toughness parameters of concrete and size effect analysis. Engng Frac Mech 2011;78:2115–38.

12 Jansen DC, Weiss WJ, Schleuchardt SHF. Modified testing procedure for the two parameter fracture model for concrete. In: The Proceedings of the 14th Engineering Mechanics Conference (EM2000): Austin, TX. May. 2000.

13 Alam MR, Azad MAK, Kadir MA. Fracture toughness of plain concrete specimens made with industry-burnt brick aggregates. Journal of Civil Engineering (IEB) 2010;38:81-94.

14 Refai TME, Swartz SE. Fracture behavior of concrete beams in three-point bending considering the influence of size effects. Report No. 190, Engineering Experiment Station, Kansas State University; 1987.

15 Go CG, Swartz SE. Energy methods for fracture-toughness determination in concrete. Exp Mech 1986;26:292–6.

16 Karihaloo BL, Nallathambi P. Fracture toughness of plain concrete from three-point bend specimens. Materials and Structures/Matériaux et Constructions 1989;22:185-93.

17 Heskandari H, Muralidhara S, Raghu Prasad BK, Venkatarama Reddy BV. Size effect in self consolidating concrete beams with and without notches. Sādhanā 2010;35:303-17.

18 Bažant ZP, Gettu R, Kazemi MT. Identification of nonlinear fracture properties from size effect tests and structural analysis based on geometry-dependent R-curves. Int J Rock Mech Min Sci & Geomech Abstr 1991;28:43-51.

19 Bažant ZP. Concrete fracture models: testing and practice. Engng Frac Mech 2002;69:165-205.

20 Wu Z, Yang S, Hu X, Zheng J. An analytical model to predict the effective fracture toughness of concrete for three-point bending notched beams. Engng Frac Mech 2006;73:2166-2191.

21 Yang ST, Hu XZ, Wu ZM. Influence of local fracture energy distribution on maximum fracture load of three-point-bending notched concrete beams. Engng Frac Mech 2011;78:3289-3299.

Figures

Figure 1. Example of a typical load-displacement relationship for concrete in a SE(B) fracture toughness test [1].

Figure 2. Schematic presentation of the fracture process of concrete. The initial crack length is a_0 and the macroscopic extended crack is Δa. PZ is the size of the active fracture process zone.

Figure 3. Schematic definition of the difference between an ideally brittle and a quasibrittle material.

Figure 4. Effective crack growth corresponding to maximum load for standard SE(B) and C(T) specimens.

Figure 5. Comparison between Bažant size effect expression and simple K-R curve size effect.

Figure 6. Comparison of Bažant size effect expression and simple K-R curve size effect for concrete and mortar representing SE(B) specimens with a constant initial a_0/W ratio [7]. The process zone size for mortar is, based on the smaller power, smaller than for concrete.

Figure 7. The effect of degradation by Calcium Leaching on the fracture behaviour and effective K-R curve of concrete SE(B) specimens with a constant a_0/W ratio [10].

Figure 8. Comparison of Bažant size effect expression and simple K-R curve size effect for concrete C(T) specimens with variable thickness and a constant a_0/W ratio [11].

Figure 9. Use of the power-law K-R expression to describe the effect of crack length on the maximum load. Data taken from [12] (a) and [13] (b).

Figure 10. The maximum load for four different specimen sizes with four different initial crack lengths are all described by a single K-R curve [2].

Figure 11. The maximum load for three different specimen sizes with strongly varying initial crack lengths are all described by a single K-R curve. The data has been taken from [14]. The squares marked by a cross are from [15], but their behaviour is practically identical to the other specimens.

Figure 12. Estimate of effective crack length at maximum load, Eq. (6), compared to Karihaloo and Nallathambi experimental data from SE(B) specimens with varying S/W [16].

Figure 13. Comparison of Bažant size effect expression and simple K-R curve size effect for concrete (a) and mortar (b) representing DEC(T) specimens with a constant initial a_0/W ratio [7]. The low constraint DEC(T) geometry produces a larger process zone than the high constraint SE(B) geometry (See Fig. 6) and this is reflected in the form of a steeper effective K-R curve. The process zone size for mortar is, based on the smaller power, for both specimen geometries smaller than for concrete.

Figure 14. Effective initial crack length corresponding to an unnotched SE(B) specimen based on cracked specimen data. Data taken from [17].

Figure 15. The prediction of load displacment dependence up to maximum load, based on simple effective K-R curve fitting to maximum load data. Data taken from [18].

Figure 16. Normalisation of effective crack driving force versus effective crack growth for self-similar SE(B) specimens of different size. Data extracted from [1]. Fig. 16a shows the effective crack driving force versus absolute effective crack growth and Fig. 16b shows the effective crack driving force versus proportional crack growth. Also included in the plots is the effective K-R curve estimated for the maximum load values in Fig. 7a.

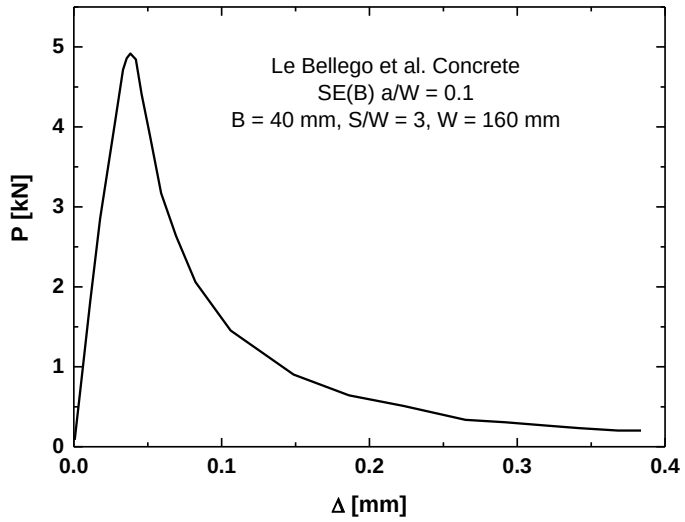

Figure 1. Example of a typical load-displacement relationship for concrete in a SE(B) fracture toughness test [1].

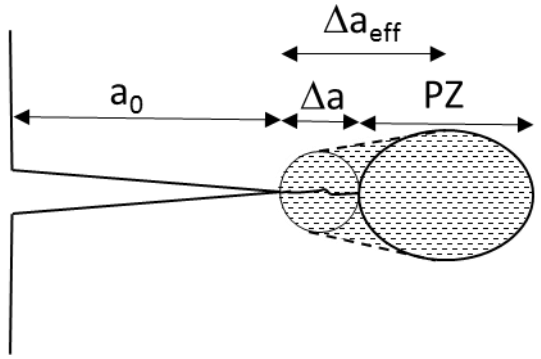

Figure 2. Schematic presentation of the fracture process of concrete. The initial crack length is a_0 and the macroscopic extended crack is Δa. PZ is the size of the active fracture process zone.

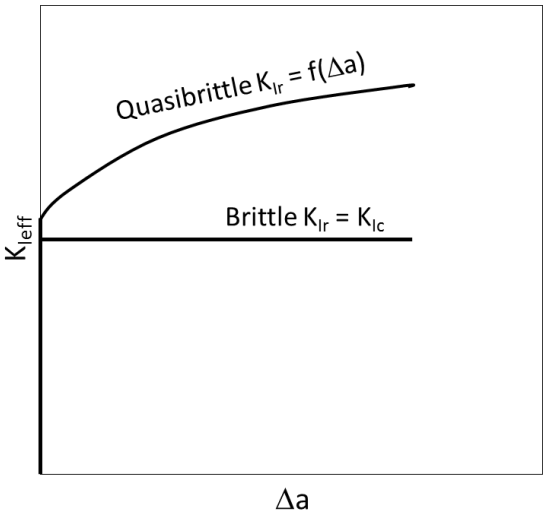

Figure 3. Schematic definition of the difference between an ideally brittle and a quasibrittle material.

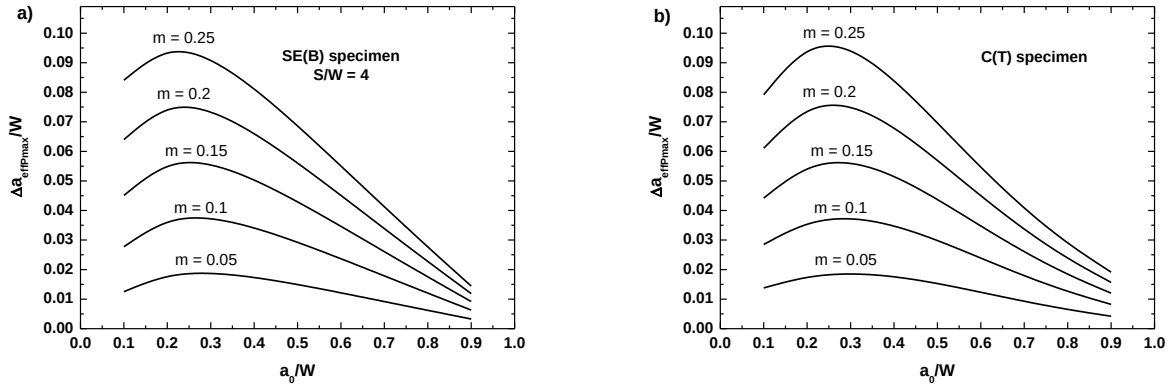

Figure 4. Effective crack growth corresponding to maximum load for standard SE(B) and C(T) specimens.

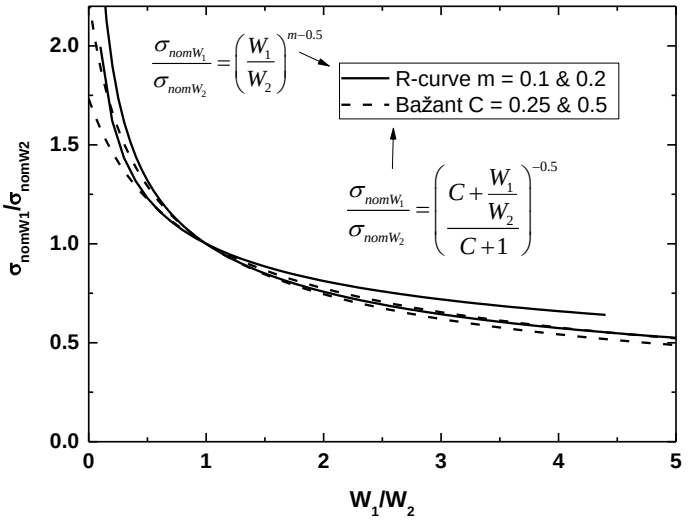

Figure 5. Comparison between Bažant size effect expression and simple K-R curve size effect.

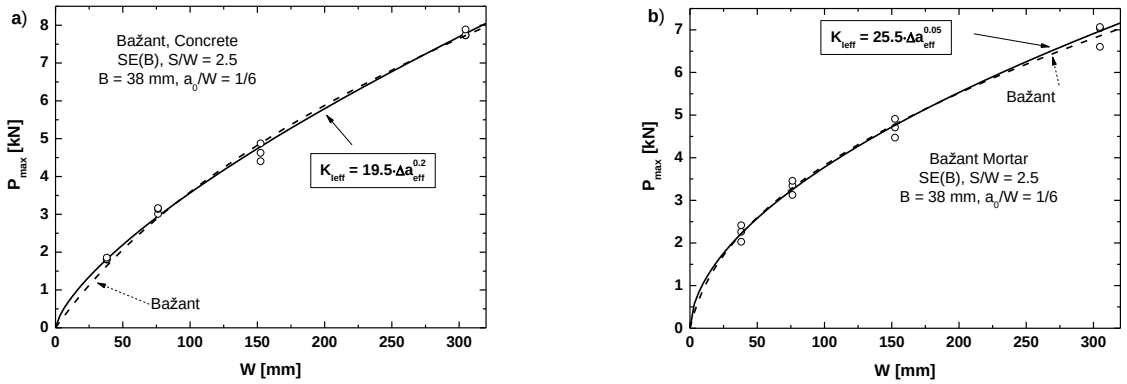

Figure 6. Comparison of Bažant size effect expression and simple K-R curve size effect for concrete and mortar representing SE(B) specimens with a constant initial a_0/W ratio [7]. The process zone size for mortar is, based on the smaller power, smaller than for concrete.

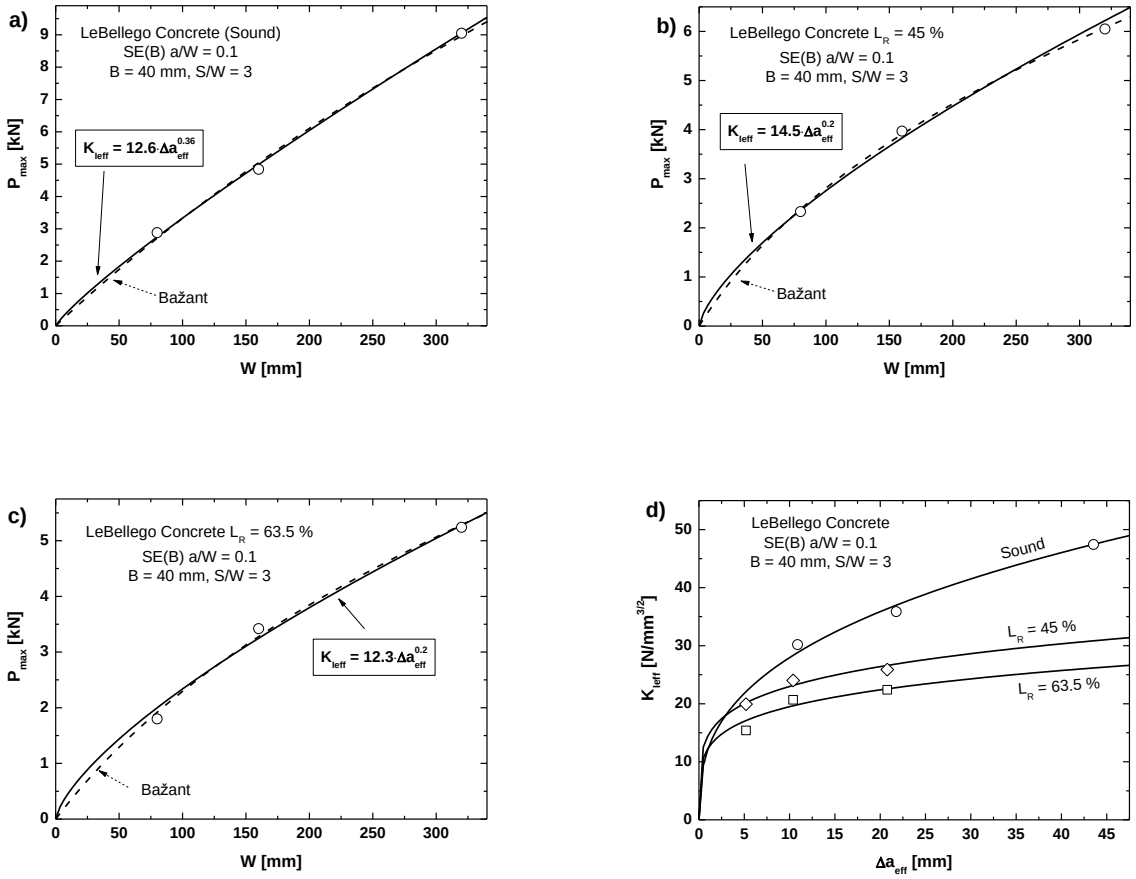

Figure 7. The effect of degradation by Calcium Leaching on the fracture behaviour and effective K-R curve of concrete SE(B) specimens with a constant a_0/W ratio [10].

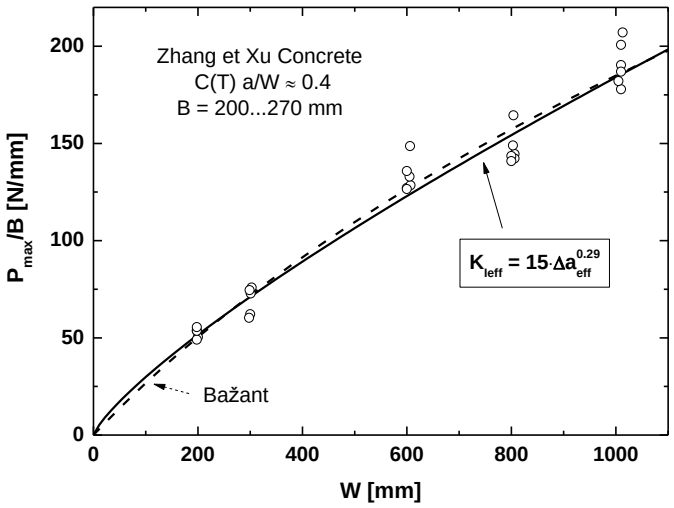

Figure 8. Comparison of Bažant size effect expression and simple K-R curve size effect for concrete C(T) specimens with variable thickness and a constant a_0/W ratio [11].

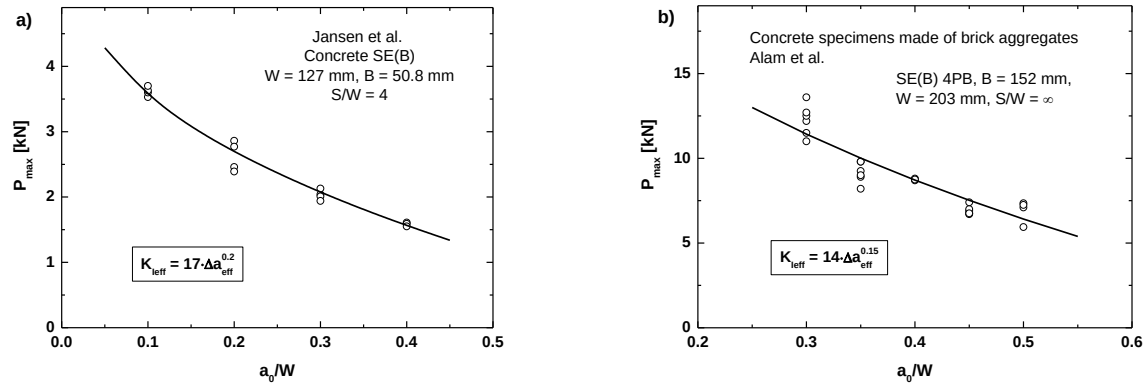

Figure 9. Use of the power-law K-R expression to describe the effect of crack length on the maximum load. Data taken from [12] (a) and [13] (b).

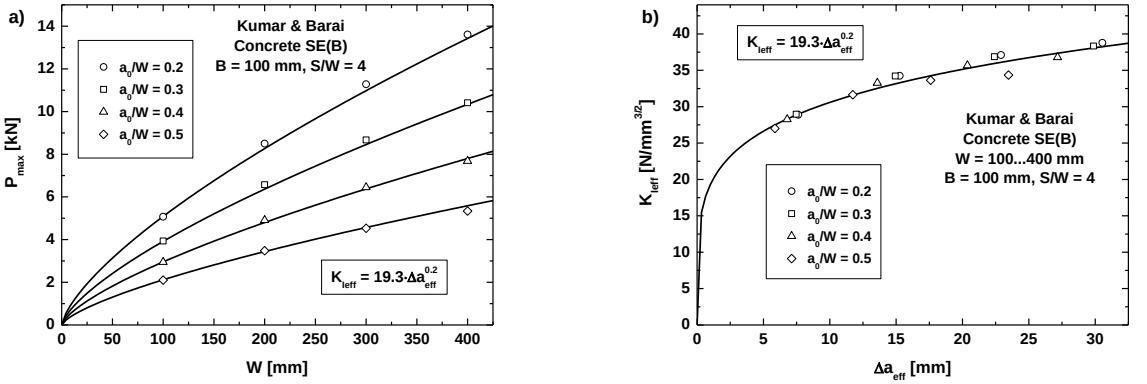

Figure 10. The maximum load for four different specimen sizes with four different initial crack lengths are all described by a single K-R curve [2].

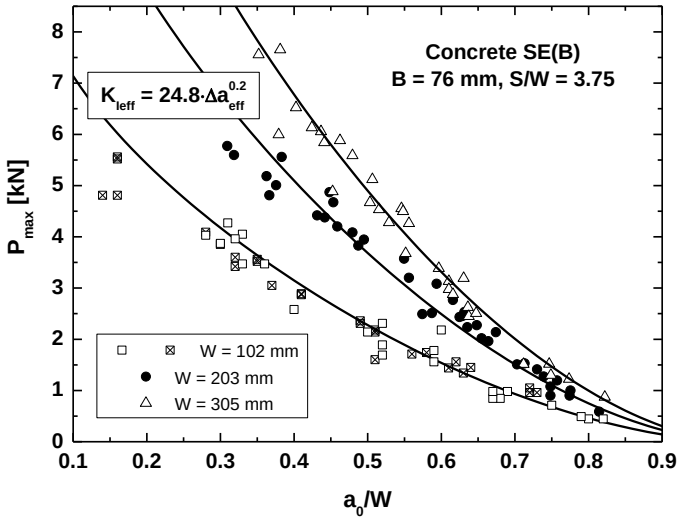

Figure 11. The maximum load for three different specimen sizes with strongly varying initial crack lengths are all described by a single K-R curve. The data has been taken from [14]. The squares marked by a cross are from [15], but their behaviour is practically identical to the other specimens.

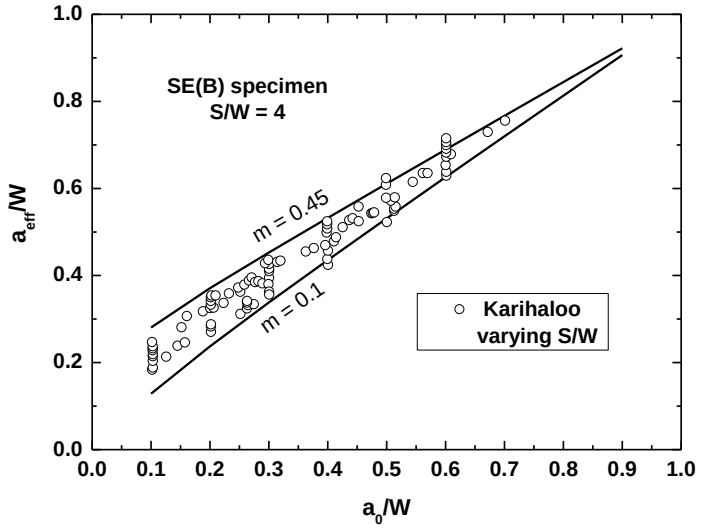

Figure 12. Estimate of effective crack length at maximum load, Eq. (6), compared to Karihaloo and Nallathambi experimental data from SE(B) specimens with varying S/W [16].

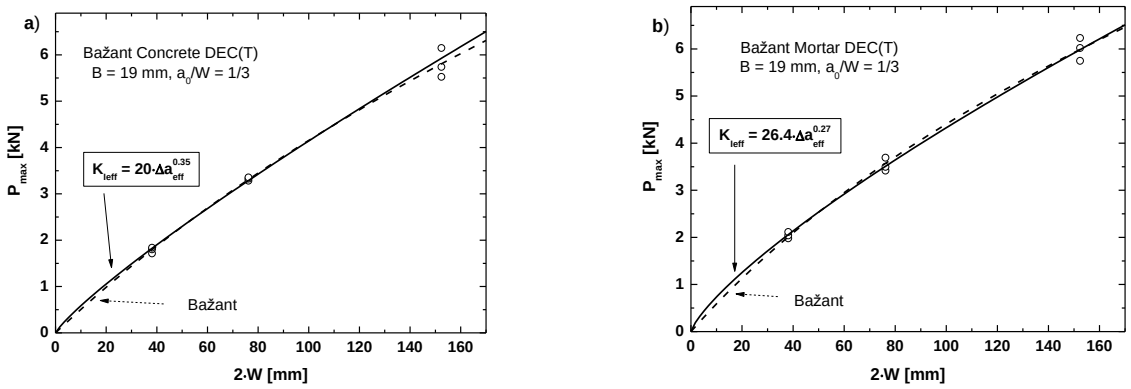

Figure 13. Comparison of Bažant size effect expression and simple K-R curve size effect for concrete (a) and mortar (b) representing DEC(T) specimens with a constant initial a_0/W ratio [7]. The low constraint DEC(T) geometry produces a larger process zone than the high constraint SE(B) geometry (See Fig. 6) and this is reflected in the form of a steeper effective K-R curve. The process zone size for mortar is, based on the smaller power, for both specimen geometries smaller than for concrete.

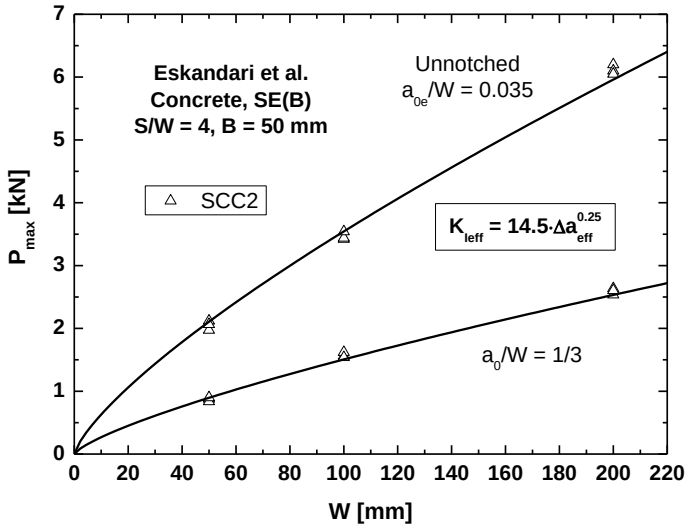

Figure 14. Effective initial crack length corresponding to an unnotched SE(B) specimen based on cracked specimen data. Data taken from [17].

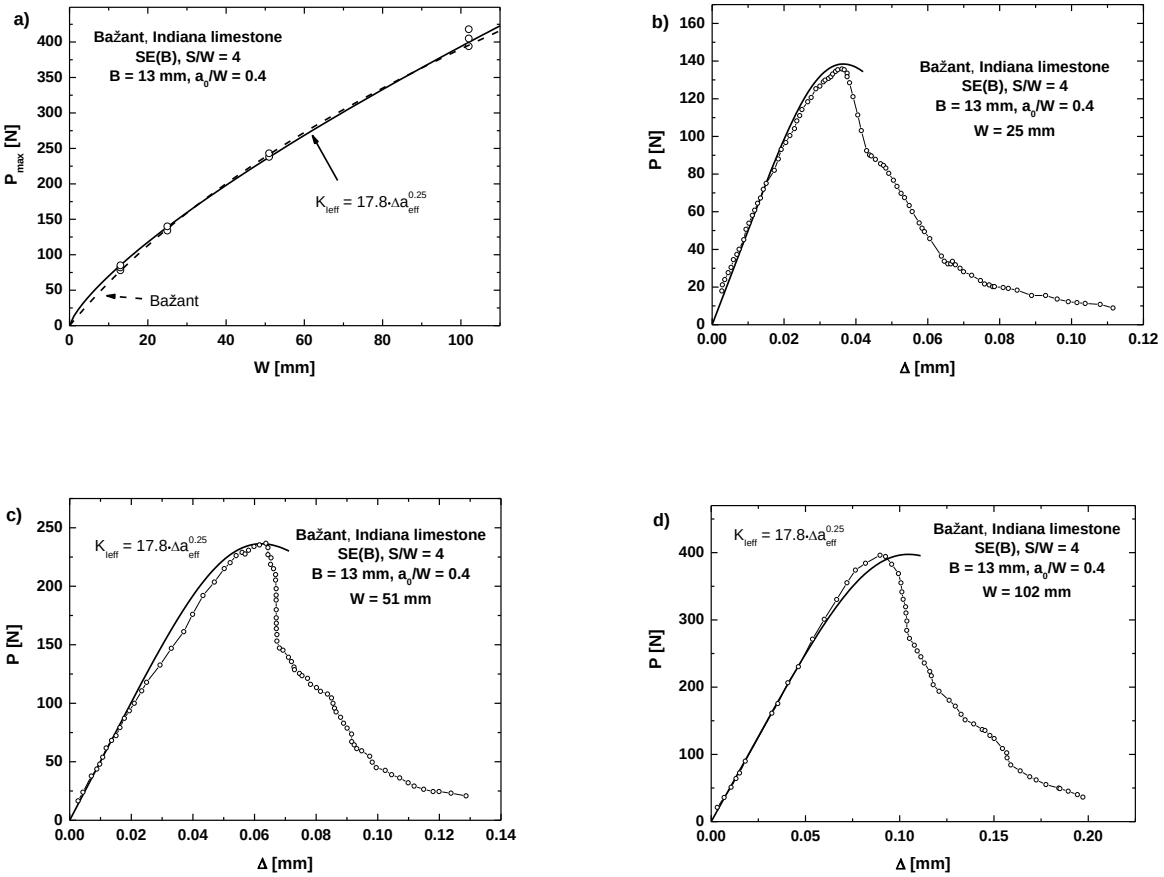

Figure 15. The prediction of load displacment dependence up to maximum load, based on simple effective K-R curve fitting to maximum load data. Data taken from [18].

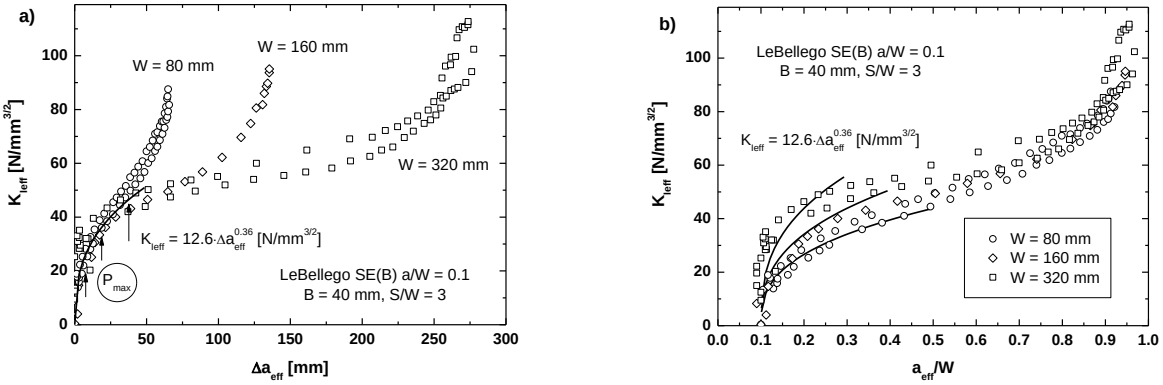

Figure 16. Normalisation of effective crack driving force versus effective crack growth for self-similar SE(B) specimens of different size. Data extracted from [1]. Fig. 16a shows the effective crack driving force versus absolute effective crack growth and Fig. 16b shows the effective crack driving force versus proportional crack growth. Also included in the plots is the effective K-R curve estimated for the maximum load values in Fig. 7a.